Applied Catalysis B: Environmental 84 (2008) 204–213

Contents lists available at ScienceDirect

Applied Catalysis B: Environmental

journal homepage: www.elsevier.com/locate/apcatb

Characterisation and catalytic activity in de-NO_x reactions of Fe-ZSM-5 zeolites prepared via ferric oxalate precursor

Mickaël Rivallan [a,b], Gloria Berlier [a,*], Gabriele Ricchiardi [a], Adriano Zecchina [a], Mircea-Teodor Nechita [c], Unni Olsbye [d]

[a] Università di Torino, Dipartimento di Chimica Inorganica Fisica e dei Materiali, Via P. Giuria 7, 10125 Torino, and NIS Centre of Excellence, University of Torino, Italy
[b] Université de Rennes1, UMR CNRS 6226, Matériaux Inorganiques: Chimie Douce et Réactivité, Campus de Beaulieu, 35042 Rennes Cedex, France
[c] Technical University "Gh. Asachi" Iasi, Faculty of Chemical Engineering, 71A, Dimitrie Mangeron Blvd., Iasi 700050, Romania
[d] inGAP Center of Research-Based Innovation, Department of Chemistry, University of Oslo, P.O. Box 1033, Blindern, N-0315 Oslo, Norway

ARTICLE INFO

Article history:
Received 15 February 2008
Received in revised form 27 March 2008
Accepted 28 March 2008
Available online 9 April 2008

Keywords:
Fe-ZSM-5
FTIR
UV–vis
Nitric oxide
Selective catalytic reduction

ABSTRACT

This paper deals with the spectroscopic characterisation and catalytic activity of Fe-ZSM-5 samples prepared by aqueous exchange with ferric oxalate and Mohr salt as precursors. NH_4^+-ZSM-5 zeolites with different Si/Al ratios were employed as starting materials, as such and after Na^+-exchange. The catalytic activity of the samples was tested in the selective catalytic reduction of NO with propane in the 473–773 K range, and the nature of extraframework Fe species was investigated by UV–vis and FTIR spectroscopies, using NO as a probe molecule. The catalytic activity was found to be dependent upon the exchange method, the Si/Al ratio and the presence of Na^+ ions. The results are discussed in terms of the relative concentration of isolated and clustered sites, as estimated by spectroscopic analysis. We propose that isolated sites are active in SCR, while clustered sites favour propane oxidation, having a detrimental effect on the activity for NO activation.

1. Introduction

Fe-containing zeolites, in particular the MFI structure (ZSM-5), have been the subject of hundreds of publications during the last decade, since the discovery in 1992 by the group of Panov of their catalytic activity in the one-step selective oxidation of benzene to phenol using N_2O as oxidising agent [1]. The catalysts initially studied by Panov were mainly Fe-ZSM-5 and Fe-silicalite [2] samples where iron was introduced in framework positions during the synthesis. Subsequent thermal treatments, necessary for catalyst activation, caused the migration of Fe from framework positions, generating extraframework Fe sites responsible for the catalytic activity [3–10]. In 1997 the first report about the activity and stability of "over-exchanged" Fe-ZSM-5 as selective catalytic reduction (SCR) catalysts for NO_x removal was reported by Feng and Hall [11], giving fresh impetus to the study of Fe in zeolites as testified by the large number of papers published on the subject [12–23].

Two parallel scientific debates about Fe-zeolites flourished in literature, devoted to the understanding of the nature of sites active in selective oxidation and of those working in SCR reactions. A huge effort was devoted to the preparation of catalysts with high activity and selectivity, especially when the method proposed by Feng and Hall [11], based on aqueous exchange with ferrous oxalate, was found not to give reproducible results [24]. The research activity was thus concentrated on two main subjects: (i) Fe-MFI samples prepared by isomorphous substitution and the role of activation procedures to increase the number of active sites [3,7], and (ii) Fe-exchanged samples and the optimisation of exchange procedures to obtain active and stable catalysts in a reproducible manner. Many different exchange procedures by solid, liquid and gas phase were proposed and studied [16,24–32].

The reasons for the large number of papers devoted to the subject, and for the lively scientific debate about the nature of extraframework Fe sites in zeolites are various. First, these systems can be considered as biomimetic ones (in particular when selective oxidation reactions are considered), showing similarities with enzymes (heme or non-heme) [33,34]. Secondly, all Fe-containing samples (both prepared by isomorphous substitution or post-synthesis ionic exchange) usually present a complex mixture of Fe sites with different nuclearity (from isolated to oxidic clusters, passing through dimers and small oligomers), different oxidation

* Corresponding author. Present address: Ecole Polytechnique Fédérale de Lausanne (EPFL), GGRC-ISIC, Station 6, CH-1015 Lausanne, Switzerland.
Tel.: +39 0116707856; fax: +39 0116707953.
E-mail address: gloria.berlier@unito.it (G. Berlier).

0926-3373/$ – see front matter © 2008 Elsevier B.V. All rights reserved.
doi:10.1016/j.apcatb.2008.03.020

(Fe^{2+}, Fe^{3+} and if possible Fe^{4+} [35]) and coordination state, as pointed out by several authors [3,36–39] This complexity is the main reason for the low reproducibility of the results, and thus for the different conclusions about the nature of the active sites reached by different research groups, as summarized in the recent and concise review of Zecchina et al. [34].

Ideally, the more homogeneous Fe sites distribution should be obtained by careful thermal activation of isomorphously substituted samples with low Fe amount, minimizing the tendency of iron to form clusters [40]. However, we showed how also in this kind of samples the distribution of Fe sites is strongly dependent upon iron content and activation conditions (temperature, ramp rate, oxidizing/reducing atmosphere etc.) [3]. The situation is typically even more complicated when Fe-exchanged samples are prepared, due to the intrinsic tendency of iron to form aggregates in solution, to diffusion problems of iron precursors inside the zeolite pores, and to the presence of residual chlorine atoms when $FeCl_2$ or $FeCl_3$ are used [24,41].

Several groups recently came to the common conclusion that two kinds of Fe sites with different specific activity are contributing to N_2O decomposition (which is used as a test reaction for selective oxidation) [8,38,42–45] and in SCR of NO_x [46]. More in detail, isolated Fe^{2+} sites were found to be selective for benzene conversion to phenol [40] and SCR reactions [46], while oligomeric and clustered species were hypothesised to limit the catalyst performance in both reactions favouring the total oxidation of benzene [40] and of the SCR reductants [46].

To reach final conclusions on this complex subject, the recent tendency of many research groups is to prepare and test "model system" samples where the complexity of Fe sites is reduced, by favouring the presence of only one type of site [47–50]. Along this line, we recently reported a new exchange method based on the use of ferric oxalate solutions [49].

In the present work, three NH_4^+ and Na^+-ZSM-5 samples with different Si/Al ratios were exchanged with the new ferric oxalate method, characterised by FTIR and UV–vis spectroscopies, and tested in the SCR of NO_x with propane, under conditions similar to those reported previously in [51]. The effect of Na^+ exchange [52] on the dispersion of iron and its activity was also considered. The activity of the samples was compared to that of samples prepared by starting from Mohr salt aqueous solution as recently reported [41].

2. Experimental

2.1. Parent zeolites

Three parent NH_4-ZSM-5 zeolites with different Si/Al ratios (nominally Si/Al = 15, 40 and 140, Na_2O = 0.05% wt) were supplied by Zeolyst International. The samples showed a surface area around of 400 (Si/Al = 15 and 140) and 425 m^2/g (Si/Al = 40) and crystal size centred around 500 nm. Na-exchanged samples were prepared by aqueous exchange of the parent zeolites with a dilute $NaNO_3$ solution following the method proposed in Ref. [52]. All Fe-exchanged ZSM-5 zeolites reported in this work have been prepared by aqueous exchange employing two different iron salts.

2.2. Ferric oxalate $Fe_2(C_2O_4)_3$

A 0.01 M solution of iron(III) oxalate was prepared using $Fe_2(C_2O_4)_3{\cdot}6H_2O$ (99%, Aldrich) in deionised water. The exchange procedure was initially performed on small amounts (0.3 g) of NH_4^+ and Na^+ zeolites, by adding to the zeolites the freshly prepared ferric oxalate solution (5 ml). During the impregnation, the iron(III) oxalate solution as well as the zeolite slurries were carefully kept away from light, in order to avoid the photochemical reduction of Fe^{3+} to Fe^{2+} and the precipitation of FeC_2O_4, a well-known process with applications in hydrometallurgy [53], following the reaction:

$$2Fe^{3+} + C_2O_4^{2-} + h\nu \rightarrow 2Fe^{2+} + 2CO_2$$

and the successive precipitation of FeC_2O_4. The pH of the 0.01 M iron(III) oxalate is 2.47, after the exchange of NH_4-zeolites a small increase was measured to pH ≅ 2.7 [49]. When Na-zeolites were employed, a sudden increase to pH 4.5 was observed, decreasing to values lower than 3 when the exchange process was completed. After 24 h the mixtures were filtered, washed with deionised water, dried in atmosphere and used for further investigations.

In order to check the reproducibility of the method and to perform catalytic tests, larger amounts of Fe-ZSM-5 (3 g) were prepared using the same procedure. The reproducibility of the method was checked by ICP analysis and FTIR spectroscopy. Elemental analysis of samples prepared from different batches showed Fe contents around 0.3–0.4 wt% in samples Fe–NH_4–Z with Si/Al = 15 and 40 and around 0.2 wt% in samples with Si/Al = 140, irrespective of the exchanged cations. Values around 0.5 wt% were measured in samples Fe–Na–Z with Si/Al = 15 and 40. FTIR spectroscopy in the OH stretching region showed in all cases a low exchange degree, varying between 10 and 30% depending on the parent zeolite. FTIR spectra of adsorbed NO were employed as routine characterisation technique on all samples. The obtained spectra were found to be highly reproducible, when using the same parent zeolites, in terms of overall intensity and of relative intensity of the different components.

The catalysts prepared by this procedure (white or slightly yellow) will be labelled as Fe–NH_4–Z_x(O) and Fe–Na–Z_x(O) (x = 15, 40, 140), respectively.

2.3. Mohr salt precursor $Fe_2(NH_4)_2(SO_4)_3$

NH_4-ZSM-5 parent zeolites (Si/Al = 15 and 40) were exchanged using Mohr salt $Fe_2(NH_4)_2(SO_4)_3$ as precursor in aqueous solution at 353 K following Ref. [41]. The initial pH of the Mohr salt solution was found to be 5.3, slightly decreasing to 4.76 after adding the zeolite. After 24 h stirring a decrease of the solution pH to 2.56 was observed. The catalysts were obtained by filtration of the suspended solution after 24 h stirring, washed with deionised water and dried in atmosphere. These samples (exhibiting an intense orange colour) will be referred to as Fe–NH_4–Z_x(M) (x = 15 and 40).

2.4. Catalysts characterisation

The IR experiments were performed on a Bruker IFS 66 FTIR instrument equipped with a cryogenic MCT detector and running at 2 cm^{-1} resolution. All the samples under study were in form of self-supporting pellets suitable for measurements in transmission mode. Before NO dosage the sample wafers were typically activated in vacuo at 773 K for 1 h directly in the IR measurement cells. Pure NO, freshly distilled from a NO_x mixture, was dosed on the activated sample at room temperature. After the first dose (P_{NO} = 15 Torr), NO was left in contact with the sample for 1 h, and the evolution of the spectra with time was followed by IR (not reported). Finally a sequence of FTIR spectra was recorded by gradually reducing the NO equilibrium pressure in the cell until $P_{NO} = 10^{-3}$ Torr. The intensity of the FTIR spectra was "normalized" in terms of thickness of the zeolite pellet by measuring the intensity of the overtone bands in the 2100–1550 cm^{-1} range, which is proportional to the quantity of the siliceous matrix in the IR beam.

UV–vis measurements were performed on a Cary 5 spectrophotometer (Varian) equipped with a Diffuse Reflectance accessory.

Spectra were measured in reflectance mode and converted into the Kubelka–Munk function $F(R)$ which is proportional to the absorption coefficient for sufficiently low $F(R)$ values. Before UV–vis measurement the samples (when necessary) were thermally treated in vacuo and oxidised under static conditions with 10 Torr of O_2. Treatments were performed in the quartz cells used for the measurements in controlled atmosphere.

Chemical composition was determined by elemental analysis, by means of a Varian Vista Pro Axial ICP spectrometer. Fe-standard solutions were made from Spectrascan-standard (1000 ppm) delivered by Teknolab.

2.5. Catalytic tests

For catalytic tests, the samples (0.32 g, 0.25–0.42 mm particle size) were mixed with quartz (0.32 g, 0.25–0.42 mm particle size) and loaded into a tubular quartz fixed bed reactor with inner diameter 10 mm. The reaction temperature was monitored by using a thermocouple placed inside a quartz thermocouple well (outer diameter 3 mm) which was inserted axially into the catalyst bed. Prior to reaction, the catalyst was heated to 773 K in an Ar stream (55 Nml/min) before it was cooled to 473 K and tested for catalytic activity at 473–573–673 and 773 K. The feed gas consisted of 447 Nml/min NO in He (1140 ppm NO, 447 Nml/min), 0.45 Nml/min C_3H_8 and 2.25 Nml/min O_2, yielding a total flow rate of 450 Nml/min (GHSV = 90,000 ml/g h^{-1} at NTP). The test duration at each temperature was 30 min, followed by switching to the Ar stream and heating to the next test temperature (dT = 5 K/min) before switching back to the reactant flow. A stability test, consisting of two subsequent test cycles at 473–573–673–773 K was performed using a 1020 ppm NO/He gas (500 Nml/min), all other conditions being equal to the preceding tests, resulting in a GHSV = 100,000 ml/g h^{-1} at NTP.

Feed and product analysis was performed by using a Pfeiffer OmniStar quadrupole Mass Spectrometer, monitoring the following ionic masses: (m/e) = 4 (He), 18 (H_2O), 28 (N_2, CO, C_2H_4), 30 (NO), 32 (O_2), 40 (Ar), 42 (C_3H_6), 44 (N_2O, CO_2, C_3H_8), 46 (NO_2). Due to overlap between characteristic masses of several products, NO conversion was calculated from the intensity of the characteristic m/e(NO) = 30 signal in the reactor feed and effluent, respectively, using He as internal standard:

$$NO_{conversion} = 100\% \times \frac{(C_{NO,feed} - (C_{NO,effluent} \times C_{He,feed}/C_{He,effluent}))}{C_{NO,feed}}$$

O_2 conversion was calculated accordingly.

3. Results and discussion

3.1. Exchange mechanism in ferric oxalate solutions

One of the ways to insert Fe^{n+} ions inside zeolitic channels is to exchange the NH_4^+ (or Na^+) ions stabilizing the negative charge induced in the framework by the presence of Al. It is well known that the exchange with Fe^{2+} and Fe^{3+} ions in the zeolite is not an easy task, due to the low stability of the +2 oxidation state and to the tendency of iron to form dimeric couples that can act as nucleation centres for larger aggregates. Moreover, since the Si/Al ratio in ZSM-5 is usually high, it could be argued that it is statistically difficult to have two negative charges in the framework close enough to stabilize Fe^{2+} or even Fe^{3+} ions. On this basis, several authors proposed that the iron ions involved in the exchange process have to be monovalent: $[Fe^{2+}(OH)]^-$, $[Fe^{3+}(OH)_2]^-$, $[Fe^{2+}Cl]^-$ etc.

The speciation of ferric and ferrous cations in oxalate solutions has been extensively studied [54] since oxalic acid is one of the best reagents for iron oxides dissolution from sand and other minerals [55]. There are several parameters that govern Fe^{3+} speciation in oxalic acid such as: pH, temperature, oxalic acid concentration, and presence of Fe^{2+} or other impurities. It was found that the optimum pH range for iron oxides dissolution is 2.5–3.0 [56,55]. The pH measured during our exchange of NH_4-zeolites with the 0.01 M solution was found to be in this range. According to speciation diagram of oxalato–Fe(III) complexes [57] the iron species that can be found in solution are: $FeHC_2O_4^{2+}$, $FeC_2O_4^+$, and $Fe(C_2O_4)_2^-$, and the formation of any types of iron precipitates can be avoided [54,57]. The only monovalent ion, $FeC_2O_4^+$, is present in small amount, so that we can assume a controlled 1:1 exchange with the zeolitic counterions M^+ ($M = H^+$, NH_4^+). When Na^+-exchanged zeolites were used as starting materials, however, a pH value of 4.5 was measured immediately after adding the oxalate solution. This pH value can be explained with a back-exchange of Na^+ ions with H_3O^+ from aqueous solution (see below, Section 3.2), so that in this case the formation of colloidal solutions of FeOOH and/or $Fe(OH)_3$ cannot be totally discarded.

Upon thermal activation at 773 K under vacuum, the organic part of the mono-oxalatoiron(III) ion $FeC_2O_4^+$ is decomposed leaving Fe^{n+} sites in extraframework positions. Decomposition can occur by release of CO and CO_2 molecules, leaving Fe^{3+} ions, or with release of CO_2 and reduction to Fe^{2+}. We will see in the following that after activation in vacuum a large amount of Fe^{2+} ions with high coordinative unsaturation are dispersed in the zeolite channels. These species could be present as counterions (even if this would imply the presence of two vicinal framework Al atoms even in samples with very low Al content) or, as recently proposed by Zecchina et al. for Fe-silicalite, as grafted ions [33,34]. In the following discussion, by the analysis of the decrease of intensity in the ν_{OH} region, we will assume for simplicity the presence of divalent counterions.

3.2. FTIR in the ν_{OH} region

FTIR spectroscopy in the OH stretching (ν_{OH}) region can be used to compare the exchange degree obtained from the parent zeolites (before and after Na exchange) by using the different precursors. The spectra obtained on the samples prepared starting from parent NH_4-ZSM-5 and Na-ZSM-5 with Si/Al = 40 and Si/Al = 15 are shown in Fig. 1, left and right parts, respectively. Spectra of parent zeolites (top spectra in full line) are composed by two major absorptions: a sharp peak at 3745 cm^{-1} (with a shoulder at 3720 cm^{-1}) and a band at 3610 cm^{-1}. The sharp peak at 3745 cm^{-1} represents isolated Si–OH groups on the external surface of the zeolite particles, while the band at 3610 cm^{-1} is related to Si(OH)Al Brønsted sites. On the series of samples with Si/Al = 15 an additional band at 3660 cm^{-1} is observed; this band is typically observed in ZSM-5 zeolites with high Al content and was assigned to defective Al–OH groups [58,59]. Due to the low intensity and poor spectroscopic quality of the Si(OH)Al bands obtained on the ZSM-5 sample with Si/Al = 140, those results are not reported.

After Na^+-exchange (grey lines), total consumption of Brønsted sites is observed on both samples (band at 3610 cm^{-1}). On sample with Si/Al = 15 the band assigned to defective Al–OH groups is also consumed. Notice that the bands related to Si(OH)Al groups are partially restored after exchange with ferric oxalate, indicating that, at the low pH employed in the exchange, Na ions are back-exchanged by protons. This is in agreement with the observed gradual increase in pH (see Section 2.1).

For all the samples, the Fe-exchange process can be estimated by measuring the intensity decrease of the Brønsted Si(OH)Al band at 3610 cm^{-1}, as summarised in Table 1. A comparison between the amount of iron measured by elemental analysis and the

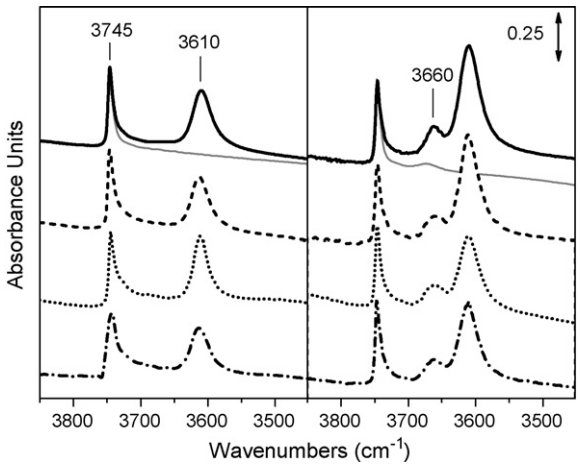

Fig. 1. FTIR spectra in the OH stretching region of Fe-exchanged samples after outgassing at 773 K. Results obtained on samples with Si/Al = 40 and 15 are reported on the left and right parts, respectively. From top to bottom: parent NH_4–Z_x (solid line), Na–Z_x (grey line); Fe–NH_4–Z_x (O) (dashed line); Fe–NH_4–Z_x (M) (dotted line) and Fe–Na–Z_x (O) (dashed–dotted line).

Table 1
Chemical composition of exchanged samples

Sample	Ion-exchange[a] (%)	Fe content[b] (wt %)	Average Fe atoms per exchanged Al(OH)Si[c]
Fe–Na–Z_{15} (O)	27.0	0.52	0.3
Fe–Na–Z_{40} (O)	21.1	0.48	1.0
Fe–Na–Z_{140} (O)	n.d.	0.20	n.d.
Fe–NH_4–Z_{15} (O)	14.7	0.37	0.4
Fe–NH_4–Z_{40} (O)	18.9	0.32	0.7
Fe–NH_4–Z_{140} (O)	n.d.	n.d.	n.d.
Fe–NH_4–Z_{15} (M)	27.0	1.03	0.6
Fe–NH_4–Z_{40} (M)	16.4	0.63	1.7

n.d., not determined due to the low intensity.
[a] Exchange degree calculated by measuring the area decrease of the IR band at 3610 cm^{-1}.
[b] Determined from ICP analysis.
[c] Calculated from Fe and Al content from elemental analysis and exchange degree from IR.

exchange degree reveals interesting differences between the materials. If, by simplicity, we assume that after the thermal treatment necessary for the activation of the sample all iron is present as bivalent counterions (Fe^{2+} or O^-Fe^{3+}), then one Fe ion should compensate two negative charges, and the ratio between Fe atoms and exchanged Si(OH)Al groups (Table 1, last column) should be 0.5. Concentrating on the Fe–NH_4–Z_x samples, the ratio in Fe–NH_4–Z_{15}(O) is rather low (0.4), indicating that the Al ions in the lattice are close enough that one Fe ion may coordinate to two lattice O^-. In Fe–NH_4–Z_{40}(O), the ratio is higher (0.7), indicating that each Fe ion coordinates to one or two lattice O^-, in compliance with the lower amount of Al in this sample. Higher values (0.6 and 1.7) are observed for the materials prepared by the Mohr salt method (Fe–NH_4–Z_{15}(M) and Fe–NH_4–Z_{40}(M), respectively), and this indicates a higher degree of Fe clustering, especially in the latter sample.

As for the Na^+-exchanged sample, the discussion is more complex, since they may still contain some Na^+. This implies that the measured ion-exchange levels could be not realistic and the introduced iron versus exchanged cations ratio (last column of Table 1) underestimated. As a consequence, the high value of this ratio in Fe–Na–Z_{40} (1.0) is a clear indication of the presence of clustering. This is in agreement with the observed increase of pH measured during the exchange, due to the back-exchange of Na+ cations with protons from the solution.

3.3. UV–visible spectroscopy of Fe dispersed on inorganic matrices

Electronic spectroscopy in the UV–visible region is a fundamental technique for the characterisation of transition metal ions dispersed on inorganic matrices. The position, shape and intensity of UV–vis bands can in fact give information on the oxidation state and symmetry of metal ions, not forgetting their aggregation state.

The more accurate information about oxidation and coordination state usually comes from bands related to d–d transitions, since these transitions were rationalized for most metal ions in terms of Ligand Field Theory. This model explains spectral features essentially involving electron transitions within orbitals located on the central ion, so that d–d transitions can be used as fingerprints for ions with well defined oxidation state in octahedral and tetrahedral coordination. As far as Fe is concerned, unfortunately, d–d bands are not easily appreciated in Fe-based heterogeneous catalysts, mainly due to the fact that transition for Fe^{3+} (d^5 configuration) are Laporte-forbidden and thus very weak. Moreover, it is very rare to have single-site catalysts (with homogeneous distribution of Fe sites with well-defined local environment), so that the rich UV–vis spectroscopy observed in Fe–biomimetic complexes cannot be easily found in inorganic systems.

Ligand-to-metal charge transfer (LMCT) transitions can also give information on the Fe structure. However Fe in tetrahedral and octahedral coordination give CT bands with similar positions, so that the use of these bands for the determination of Fe coordination state is not straightforward, as testified by the controversial literature on the subject. When Fe is concerned however, UV–vis bands can be used to estimate in a semi empirical way the metal ions clustering degree, since it is well known that the band positions shift to lower wavenumbers by increasing nuclearity, as rationalized by several groups [60–62].

3.3.1. Evolution of Fe state in samples prepared by the ferric oxalate method

In this contribution UV–vis spectroscopy is applied to study the insertion of Fe ions in zeolites by using different precursors. Moreover, the structural modifications induced by thermal treatments on the inserted Fe species was followed. Fig. 2 shows the UV–vis spectra obtained on sample Fe–NH_4–Z_{40} (O) after aqueous exchange (and subsequent drying) and after activation in vacuo and oxidation in O_2 at 773 K (full and dashed curves respectively). To help in the interpretation, the spectrum of powdered ferric oxalate (the precursor used for the exchange) is also reported (dotted curve), exhibiting three very intense broad bands at 39,600, 36,100 and 27,900 cm^{-1}. Before thermal activation (full line), the spectrum of the Fe-exchanged sample is composed by a strong and complex absorption in the 48,000–21,000 cm^{-1} range. Upon calcination (dashed line), the spectrum is transformed into an intense band with maximum at 41,000 cm^{-1} and a tail up to 20,000 cm^{-1}.

The molecular structure of $Fe_2(C_2O_4)_3$ in solid state was studied by Edwards and co-workers [63] who showed that oxalate ligands adopt a bidentate coordination so that each metal ion is linked by three oxygen atoms (see Scheme 1). On the basis of this structural evidence, we assign the three bands at 39,600, 36,100 and 27,900 cm^{-1} to LMCT bands related to isolated Fe sites in trigonal coordination.

When ferric oxalate is used for aqueous exchange (in the experimental conditions employed in this work), the $[Fe(C_2O_4)]^+$ (oxalatoiron(III) ion) is supposed to be main species involved in the ion exchange process [49,54]. The interpretation of the UV–vis spectrum of the exchanged zeolite before thermal activation is not straightforward, being sensibly different with respect to that of ferric oxalate and also of ferric oxalate solution (not reported for simplicity). We can only suggest that it is associated with the

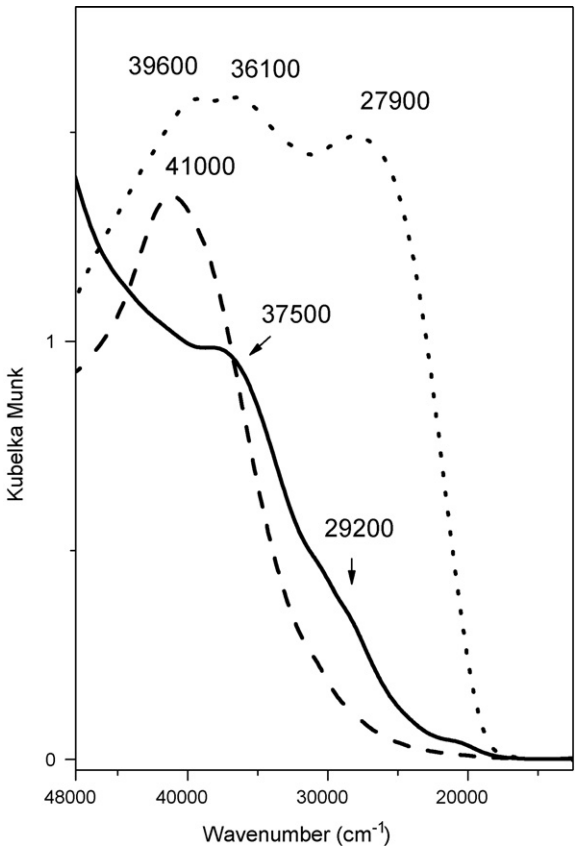

Fig. 2. UV–vis DRS spectra of sample Fe–NH_4–Z_{40} (O) measured in air after the exchange procedure (solid line) and after subsequent activation in vacuo and oxidation in O_2 at 773 K (dashed line). For comparison, the spectrum of the ferric oxalate precursor $Fe_2(C_2O_4)_3$ diluted in SiO_2, (dotted line) is reported.

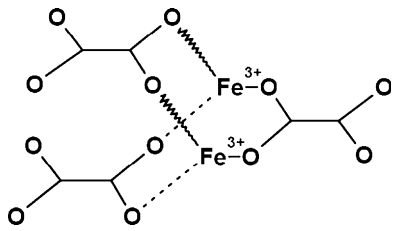

Scheme 1. Molecular structure of ferric oxalate salt proposed in Ref. [63].

species represented in Scheme 2, involving a $[Fe(C_2O_4)]^+$ ion as zeolitic counterion.

Upon calcination, the bands assigned to the oxalatoiron(III) ion interacting with the zeolite oxygen are destroyed and a new band with a maximum at 41,000 cm^{-1} is formed. Intense CT absorption in the same range was reported for isolated Fe^{3+} ions in tetrahedral coordination in inorganic crystals [64], and in the framework

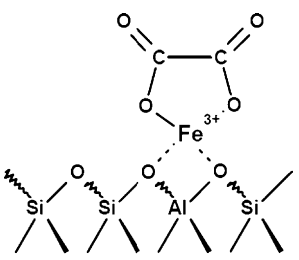

Scheme 2. Proposed structure for iron species in Fe-ZSM-5 after ion exchange with ferric oxalate [49].

positions of Fe-silicalite [60]. On this basis, we suggest that this feature is associated with the presence of isolated Fe sites, interacting with the zeolite framework as counterions [45,65,66]. These sites would be generated upon calcination by the removal of the oxalato ligand, being stabilized by the negatively charged zeolite framework.

Since the band at 41,000 cm^{-1} is characterised by a slight asymmetry to low frequency (giving a tail up to 20,000 cm^{-1}), the presence of a minimum amount of oligomeric and very small oxidic Fe_xO_y species, formed upon calcination or during the aqueous exchange, cannot be completely discarded [60–62].

3.3.2. Effect of Si/Al ratio and of the iron precursor

The UV–vis spectra reported in Fig. 3 show the influence of the aluminium content on the nature of Fe sites in samples prepared with ferric oxalate and subsequently activated. NH_4-ZSM-5 zeolites with Si/Al = 15 (full line), 40 (dashed line), 140 (dotted line) were used as starting materials. As a first remark we can observe that all samples exhibit the band at 41,000 cm^{-1}, the intensity of which decreases in the following order: 40 (dashed line), 15 (full line), 140 (dotted line). This band is well defined and narrow in Fe–NH_4–Z_{40} (O) whereas samples Fe–NH_4–Z_{140} (O) and Fe–NH_4–Z_{15} (O) show an additional component at 30,000 cm^{-1}, with a shoulder around 21,000 cm^{-1}, that seems to grow at the expense of the 41,000 cm^{-1} one. Since the latter can be interpreted in terms of isolated Fe sites, while the former is a clear indication of oligomers formation, the spectra of Fig. 3 indicate that the dispersion of Fe inside ZSM-5 channels is strongly influenced by the Al content. In fact, the sample with a negligible amount of Al (Si/Al = 140) shows weak UV–vis features and relatively large amount of oligomers, irrespective of the low iron amount (Table 1).

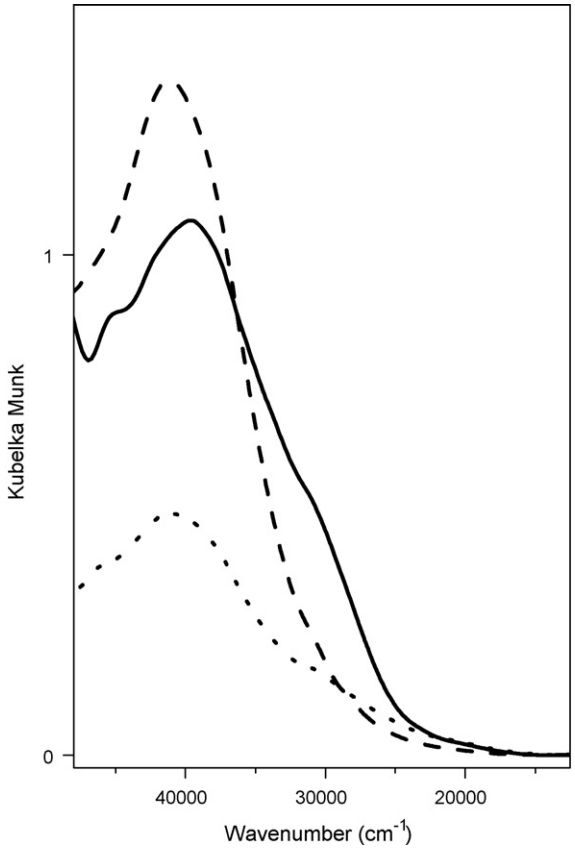

Fig. 3. UV–vis DRS spectra of samples Fe–NH_4–Z (O) at different aluminium content, Si/Al = 15 (solid line), 40 (dashed line), 140 (dotted line) after oxidation in O_2 at 773 K.

Notice that, when comparing samples Fe–NH_4–Z_{15} (O) and Fe–NH_4–Z_{40} (O), the UV–vis results are not in agreement with the indications coming by the analysis of the ν_{OH} region. The latter data in fact suggested a higher exchange degree for the Si/Al = 15, suggesting a lower amount of clustered sites. We suggest that this apparent contradiction could be explained with the assumption that the negative charges of the zeolite framework, in the samples with high Al content, can stabilize also oligomeric $[Fe_xO_y]^{n+}$ clusters, responsible for the component 30,000 cm^{-1}. This hypothesis is in agreement with the models of dinuclear clusters proposed by Battiston et al. in exchanged zeolites [28].

The UV–vis spectra reported in Fig. 4 illustrate the effect of the exchange with different iron precursors on the same parent zeolite (NH_4–Z_{40}). The spectra obtained on Fe–NH_4–Z_{40} (O) (discussed above, here reported again as dashed curve) are compared with those obtained on Fe–NH_4–Z_{40} (M) (full line) and of Fe–Na–Z_{40} (O) (dotted line). For an easier discussion, the spectra were normalized to the maximum intensity. This comparison directly allows to highlight the relative growth of clustered species (components at 30,000 and 21,000 cm^{-1}) passing from the ferric oxalate samples to the Mohr salt one, the sample prepared from ferric oxalate solutions after Na^+ exchange showing an intermediate behaviour. A similar trend was observed for samples with Si/Al = 15 and is in agreement with the amount of Fe measured by ICP analysis.

3.4. FTIR spectroscopy in the nitrosyl region 1950–1700 cm^{-1}

FTIR spectroscopy of adsorbed NO has been used by many authors [29,31] to characterise Fe-containing zeolites, due to the affinity of NO for dispersed Fe sites (especially Fe^{2+}) and to the sensitivity of the method, which allowed the characterisation of samples with Si/Fe ratios as high as 1200 [47]. In a previous work, we have shown how, when probed with NO, a large variability of Fe sites can be monitored in Fe-zeolites, their concentration being quite sensitive to small variations in preparation and activation conditions [3]. This variability is indeed one of the reasons for the different conclusions proposed in the literature by many authors. It is thus important to underline the fact that the samples prepared by the ferric oxalate method have shown a remarkable reproducibility in terms of overall and relative intensity of the observed nitrosyl bands (results not reported for brevity).

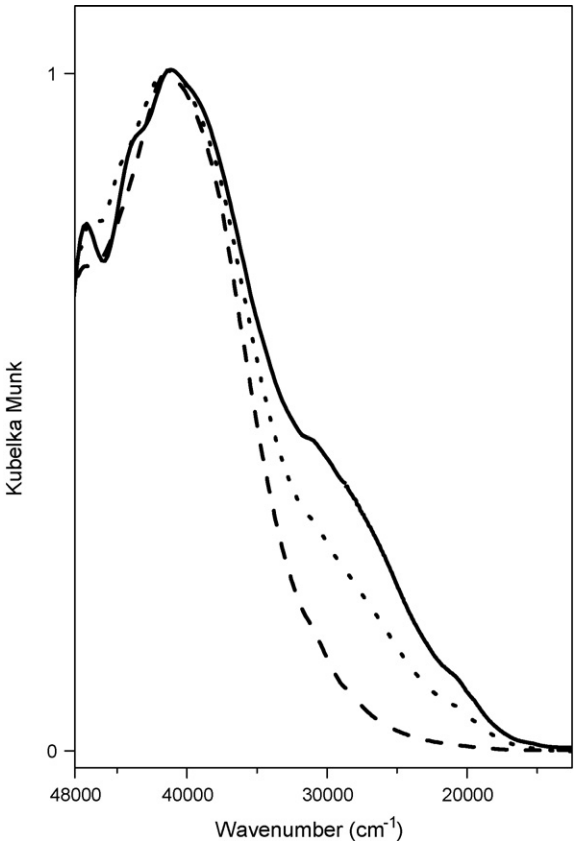

Fig. 4. UV–vis DRS spectra of Fe-exchanged zeolite with Si/Al = 40: Fe–Na–Z_{40} (O) (dotted line), Fe–NH_4–Z_{40} (O) (dashed line), Fe–NH_4–Z_{40} (M) (solid line) after oxidation in O_2 at 773 K. Spectra were normalized to the maximum intensity.

3.4.1. Effect of Si/Al ratio of parent zeolite

Fig. 5 shows the FTIR spectra of NO adsorbed at RT on the three ferric oxalate exchanged samples with different Si/Al ratios; from left to right: (a) Fe–NH_4–Z_{15} (O), (b) Fe–NH_4–Z_{40} (O) and (c) Fe–NH_4–Z_{140} (O). Before NO dosage samples were outgassed at 773 K. Spectra corresponding to the highest NO coverage (P_{NO} = 15 Torr) are reported as dotted lines, the effect of gradually decreasing P_{NO} is illustrated in full lines. Dashed lines represent the final spectra recorded at 10^{-3} Torr, after 30 min outgassing at IR beam temperature. Spectra are here shown in the typical nitrosyl region (1950–1700 cm^{-1}), while the region where vibrational modes of NO disproportionation products (N_xO_y) are usually observed (2300–2000 cm^{-1}) will be discussed in the following.

As a general remark, the overall intensity of the nitrosyl bands decreases by diminishing the Al content of the parent zeolite, being highest on sample Fe–NH_4–Z_{15} (O), and very low in sample Fe–NH_4–Z_{140} (O). This implies that framework Al favours the dispersion of various forms of extraframework Fe species inside the zeolitic channels, as evidenced by UV–vis results. Since NO probes the accessible and reactive surface Fe sites, we can use the intensity of nitrosyl bands to estimate the fraction of surface sites.

The assignment of the bands in the 1950–1700 cm^{-1} interval has been already explained in terms of mono-, di- and tri-nitrosyl complexes formed on isolated and clustered Fe^{2+} and Fe^{3+} sites [49]. This complex spectroscopy can be appreciated on sample Fe–NH_4–Z_{40} (O), in part (b) of Fig. 5. The broad absorption at 1884 cm^{-1}, quite stable upon NO desorption, was assigned to Fe^{3+}(NO) complexes formed on the surface ions of small iron clusters. In agreement with UV–vis results, we suggest that these complexes are related to iron ions in very small clusters, probably the oligomers responsible for the UV–vis component around 30,000 cm^{-1}. Surface sites of larger clusters (UV–vis band at 21,000 cm^{-1}) could also contribute to the IR feature at 1884 cm^{-1}, however in this case the fraction of surface sites should be minor.

The couple of bands absorbing at 1917/1809 cm^{-1} diminishing with NO outgassing, is related to iron sites interacting with three NO molecules, forming $Fe^{2+}(NO)_3$ species. This couple of bands is transformed upon NO outgassing in the pair at 1846–1767 cm^{-1}, proportionally increasing, and assigned to $Fe^{2+}(NO)_2$ complexes, following the equilibrium of Scheme 3:

These di- and tri-nitrosyl complexes were explained in terms of isolated Fe sites with high coordinative unsaturation, stabilized by the zeolitic surface [47].

Interesting considerations can be done by comparing the relative intensity of the bands assigned to $Fe^{2+}(NO)_3$ species (1917/1809 cm^{-1}) with that of the mono-nitrosyl formed on oligomers/clusters (1884 cm^{-1}) on samples Fe–NH_4–Z_{15} (O) and Fe–NH_4–Z_{40} (O) (parts a and b respectively). The intensity of the band at 1884 cm^{-1} is quite high in sample Fe–NH_4–Z_{15} (O), suggesting that in this sample the fraction of exposed sites in clusters is high. On the contrary isolated sites (able to add up to 3 NO molecules) represent the major fraction of surface sites in sample with Si/Al = 40. These results are in good agreement with UV–vis ones (see before).

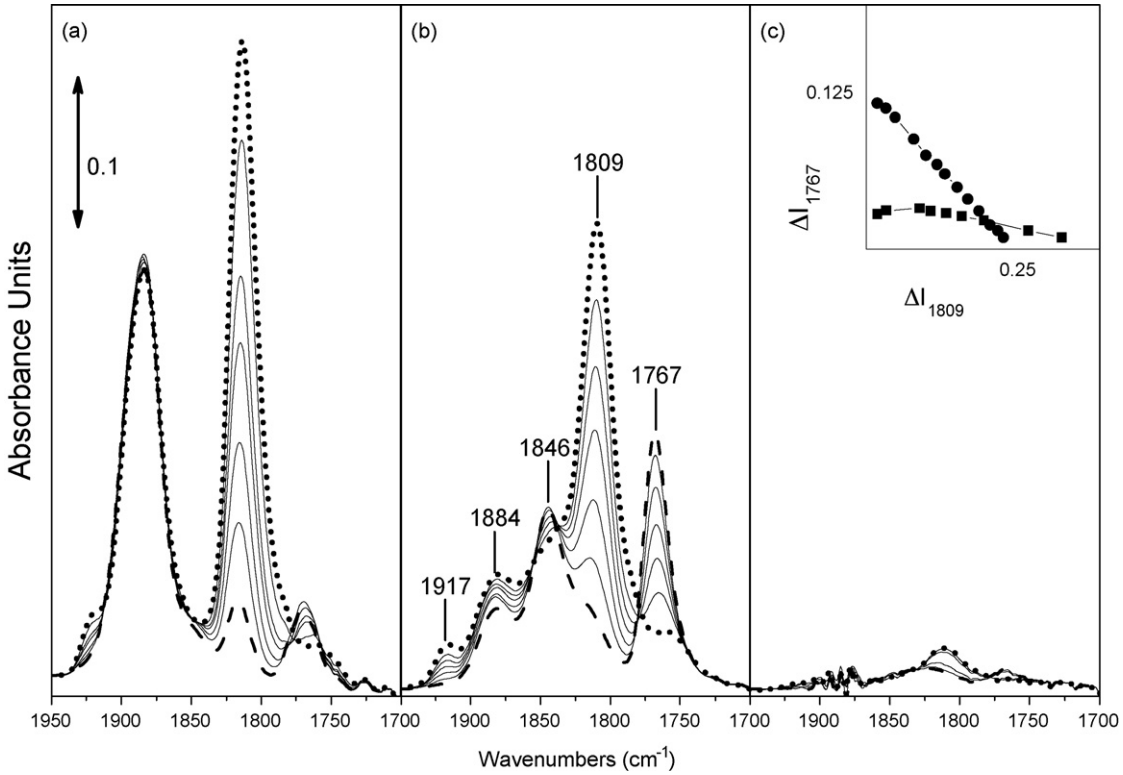

Fig. 5. FTIR spectra of NO adsorbed at room temperature on Fe–NH_4–Z (O) at different Si/Al ratio (previously outgassed at 773 K). From left to right: Si/Al = 15, 40, 140. Dotted lines, in the presence of 15 Torr of pure NO; dashed line, after outgassing for 30 min at the IR beam temperature; solid lines, intermediate NO coverages. The inset displays the intensity decrease of the band at 1809 cm^{-1} versus the increase of the component at 1767 cm^{-1} for samples Fe–NH_4–Z_x (O) with Si/Al = 15 (squares) and 40 (circles).

The spectra assigned to the $Fe^{2+}(NO)_2/Fe^{2+}(NO)_3$ equilibrium on Fe–NH_4–Z_{15} (O) sample show an evident anomaly with respect to the usual trend, which is instead exemplified by the spectra of sample Fe–NH_4–Z_{40} (O) (compare Figs. 5a and b). In fact, in sample Fe–NH_4–Z_{15} (O) the decrease of the bands at 1917/1809 cm^{-1} is not accompanied by the usual increase of the couple at 1846/1767 cm^{-1} implying that in this case the equilibrium of Scheme 3 does not hold. A similar trend was reported on Fe-silicalite samples previously oxidised and was explained in terms of ligand displacement reaction between adsorbed oxygen atoms and NO ligands [3]. What shown in Fig. 5 is however a different situation, since samples were not contacted with oxygen.

The reasons of this anomaly in sample Fe–NH_4–Z_{15} (O) are still unclear, we propose that it is related to the high Al content, causing a peculiar behaviour of the sample, as also testified by the complex spectra in the OH stretching region. One hypothesis could be that the vicinity of Al atoms (in framework tetrahedral positions or in defective Al–OH sites responsible for the band at 3660 cm^{-1}, see Fig. 1) influences the electronic properties of Fe ions and thus the stability of the di- and tri-nitrosyl complexes. A second possibility is that the observed bands are due to two distinct Fe^{2+} sites with a different number of ligands in the coordination shell.

3.4.2. Effect of iron precursor and Na^+-exchange

In the previous paragraph we have discussed the effect of Si/Al ratio on the nature and distribution of Fe sites introduced in NH_4-ZSM-5 zeolites by the ferric oxalate method. We are now going to compare these results with those obtained by using (i) Mohr salt precursor on the same parent zeolites and (ii) ferric oxalate on Na^+-exchanged zeolites. For a direct comparison of all samples, Fig. 6 reports the FTIR spectra recorded at the highest NO coverage (P_{NO} = 15 Torr) in the 2300–1700 cm^{-1} range; from top to bottom: (a) Fe–NH_4–Z_x (M), (b) Fe–NH_4–Z_x (O) and (c) Fe–Na–Z_x (O). Full line spectra correspond to Si/Al = 15, dashed to Si/Al = 40 and dotted to Si/Al = 140. In this case, close to the 1950–1700 cm^{-1} range where Fe–nitrosyl bands are usually observed, we also report the 2300–2000 cm^{-1} region, where NO disproportionation products (N_xO_y) are absorbing.

$$Fe^{2+}(NO)_3 \rightleftarrows Fe^{2+}(NO)_2$$

Scheme 3. Equilibrium with NO pressure between complexes giving bands at 1917/1809 and 1846/1767 cm-1.

Considering the bands due to nitrosyl complexes in the 1950–1700 cm^{-1} range, we observe again a relation between Al content of the parent zeolite and intensity of nitrosyl bands, as discussed above. In fact the highest band intensity generally corresponds to samples with Si/Al = 15 (full line spectra), while for very low Al contents (Si/Al = 140) the intensity is very low (dotted spectra). As far as samples with Si/Al = 15 are concerned, the spectra testify of a large concentration of isolated sites (their fingerprint being the band at 1809 cm^{-1}) but also the increase of oligomeric/clustered ones (band at 1884 cm^{-1}), in agreement with UV–vis results. Finally, the intensity of the bands obtained on samples with Si/Al = 140 is too low for any sensible consideration.

3.5. FTIR spectroscopy in the NO_x region 2300–2100 cm^{-1}

In the previous paragraph, only the bands due to Fe–nitrosyl complexes, in the 1950–1700 cm^{-1} range, were discussed. These represent the major spectroscopic manifestation when pure NO is contacted with Fe-zeolites under the experimental conditions employed. However, minor spectroscopic features can also be observed in the 2300–2000 cm^{-1} region. In this region some of the most common products related to room temperature catalytic decomposition of NO are absorbing, namely N_2O and the

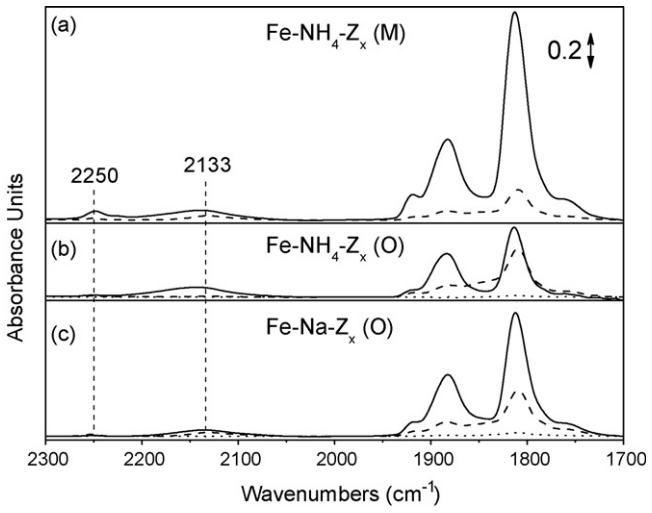

Fig. 6. FTIR spectra recorded at the highest NO coverage (P_{NO} = 15 Torr) in the 2300–1700 cm^{-1} range; from top to bottom: (a) Fe–NH_4–Z_x (M), (b) Fe–NH_4–Z_x (O) and (c) Fe–Na–Z_x (O). Solid line spectra correspond to Si/Al = 15, dashed to Si/Al = 40 and dotted to Si/Al = 140.

nitrosonium ion NO^+. It is important to underline the fact that many N_xO_y impurities (N_2O, N_2O_3 etc.) are usually present in NO cylinder, due to high pressure induced disproportionation. For this reason the NO used in our experiments is freshly distilled before use and its purity carefully checked in order to avoid misleading interpretations.

The room temperature products of NO disproportionation can be appreciated in Fig. 6 where the spectra obtained after 60 min of RT NO contact are reported for the whole series of samples under study. Close to the intense bands due to nitrosyl complexes, reaction products adsorbed on the catalyst surface are discernable in 2300–2100 cm^{-1} region, namely a broad and asymmetric absorption centred at 2133 cm^{-1} and a band at 2250 cm^{-1}. The intensity of the former is higher on samples with Si/Al = 15, followed by samples with Si/Al = 40 and 140; its intensity being hardly correlated to any of the bands in the nitrosyl region. A component at higher frequency (around 2167 cm^{-1}) is apparent in samples Fe–NH_4–Z_{15} (M) and Fe–NH_4–Z_{15} (O). Also the intensity of the narrow band at 2250 cm^{-1} is higher with Si/Al = 15, and follows the order Fe–NH_4–Z_x (M) > Fe–NH_4–Z_x (O) > Fe–Na–Z_x (O), without any evident correlation with other bands.

The nature of the band at 2133 cm^{-1}, that is not completely removed by RT outgassing, has been discussed by many authors [67–69]. Hadjiivanov et al. observed this manifestation over H-ZSM-5 zeolite upon co-adsorption of O_2 and NO. The band, which was hardly observable in absence of oxygen and was thus described in terms of an intermediate product of NO oxidation, was assigned to the nitrosonium NO^+ ion, occupying cationic positions in the zeolite channels and cavities [70,71]. A component at higher frequency was assigned by Lobree et al. to some form of $NO_2^{\delta+}$ [31], and a similar explanation was proposed by our group to explain the component at *ca* 2133 cm^{-1} formed upon NO adsorption on oxidized Fe-silicalite samples [3]. The assignment of this band and, more importantly the definition of the reaction mechanism leading to its formation are still controversial.

The assignment of the band at 2250 cm^{-1} to the formation of adsorbed N_2O is straightforward, being very similar to the bands obtained upon N_2O adsorption on Fe-silicalite (2235 and 2275 cm^{-1} assigned to N_2O adsorbed on Fe^{2+} and Fe^{3+} respectively) [72] and Fe-ZSM-5 (2226 and 2282 cm^{-1}) [73]. This species is easily desorbed from the catalyst surface by RT outgassing. To our knowledge, the formation of N_2O as RT disproportionation product of NO on Fe-zeolites is not very common, only Joyner and Stockenhuber reported a similar absorption without assigning it [14]. Spoto et al. witnessed the N_2O formation by FTIR during NO adsorption over Cu-ZSM-5 and they explained it as an unstable recombination of two NO molecules on Cu^{2+} cations [74].

A comprehensive explanation of the mechanisms leading to the formation of the bands at 2250 and 2133 cm^{-1} is outside the scopes of this work. We believe that these products are the results of many catalytic steps involving Fe–nitrosyl complexes. It is important to underline the fact that similar products are only formed on Al-free Fe-silicalite samples after oxidative treatments with O_2 or N_2O. This complex and intriguing subject will be approached with a deeper analysis in a separate publication. For the scope of this work it is sufficient to suggest that the oxidation of NO to give NO^+ could be related to the presence of active oxygen species adsorbed on Fe ions, and that the presence of Al plays an important role in this reactivity.

3.6. Catalytic activity and relations with Fe speciation

NO conversion curves versus temperature for the selective catalytic reduction of NO over activated Fe-ZSM-5 catalysts are presented in Fig. 7. Product selectivities are not reported due to overlap between various products in the mass spectrometric analysis. However, during reaction, a decrease in the NO (m/e = 30) and O_2 (m/e = 32) signals was always accompanied by a pronounced increase in the H_2O (m/e = 18), (CO + N_2) (m/e = 28) and (CO_2 + C_3H_8 + N_2O) (m/e = 44) signals, mainly representing oxidation of propane into CO_x and H_2O. The NO_2 signal (m/e = 46) was very minor, never exceeding 0.25% of the initial NO signal intensity.

When considering the results in Fig. 7, it should be noted that, at the time of starting the catalytic measurements at 473 K, each

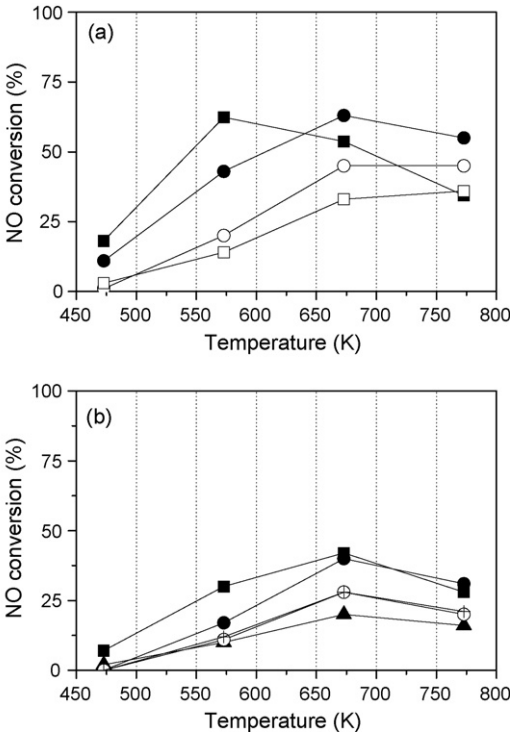

Fig. 7. Conversion of NO in the SCR with C_3H_8 on the series of Fe-exchanged samples (GHSV *ca* 90,000 ml g^{-1} h^{-1} at NTP). (a) Fe–NH_4–Z_x (O) and Fe–NH_4–Z_x (M) samples in full and open symbols, respectively; (b) Fe–Na–Z_x (O). For both parts (a) and (b), iron containing zeolites with Si/Al ratio of 15 are represented in circle, 40 in square and 140 in triangle symbols. Cross-centred symbol represents a reproducibility test of a second Fe–NH_4–Z_{15} (O) sample (GHSV *ca* 100,000 ml g^{-1} h^{-1} at NTP).

Table 2
Comparison between our results and literature data

Reference	Reductant	GHSV (ml/g/h)	O_2/C_3 ratio	NO conv. at 573 K (%)	NO conv. at 673 K (%)	NO conv. at 773 K (%)
This work (Fe–NH_4–Z_{40}–O)	Propane	90,000	5	62	54	34
Chen et al. [51]	Propane	84,000	11	60	44	26
Lobree [75]	Propane	30,000	10	23	30	14
Schwidder et al. [46]	Isobutane	42,000	11	58	88	75

catalyst sample had undergone the same treatment as before the spectroscopic measurements described in Sections 3.4 and 3.5 and Figs. 5 and 6. The results may therefore be compared directly.

Part (a) of Fig. 7 compares the NO conversion measured on the series of samples prepared by ferric oxalate (full symbols) and Mohr salt exchange (open ones) starting from NH_4-exchanged parent zeolites, while part (b) shows the results obtained on samples prepared by exchange of Na^+-zeolites with ferric oxalate. The results obtained on NH_4^+-samples with Si/Al = 140, showing a low activity in the whole temperature range, were not reported. A blank test, using SiO_2 instead of the catalyst, gave negligible conversion of NO and O_2 in the whole temperature range.

As a first general comment, a stable NO conversion with time on stream was observed over all samples at 473 K, and the conversion obtained at this temperature may therefore be taken as a measure of their initial activity.

From the results presented in Fig. 7a, it is clear that the samples prepared by the oxalate method (full symbols) are significantly more active than the samples prepared by the Mohr salt method (open ones), in spite of the higher Fe content of the latter (Table 1). Further, when comparing the results in Fig. 7(a) and (b), it is clear that the samples prepared by the oxalate method after Na exchange (Fe–Na–Z_x(O)) possess an intermediate activity between the NH_4-samples prepared by the oxalate and Mohr salt method.

For each method it is observed that the Z_{40} sample is more active than the Z_{15} sample, in spite of a similar or lower Fe content. The NO adsorption results reported in Figs. 5 and 6 show that the Z_{15} samples contain a significantly higher amount of exposed Fe sites than the Z_{40} samples. However, the relative amount of isolated Fe sites versus clustered sites is lower for the Z_{15} samples than for the Z_{40} samples, when prepared by the same method. These results clearly indicate that clustered sites are detrimental for the NO_x reduction over Fe-ZSM-5 samples, as previously suggested by Schwidder et al. [46].

The conversion–temperature curves in Fig. 7 show an increase in NO conversion with temperature in the 473–673 K temperature range, except for the most active catalyst, Fe–NH_4–Z_{40}(O), which gave a lower NO conversion at 673 K than at 573 K. At 773 K, all samples either gave similar, or lower, NO conversions compared to 673 K. When considering next the O_2 conversion curves (not shown), an increase in oxygen conversion was observed with increasing temperatures for all samples, throughout the temperature range.

It has been suggested in literature that clustered sites are active for the competing oxidation reaction, *i.e.*, propane combustion [46]. In order to elucidate whether the loss of NO selectivity at higher temperatures is related to Fe sintering, or is simply a kinetic effect, the Fe–Na–Z_{15}(O) sample was subjected to a new test, consisting of two consecutive test cycles at 473–773 K. (Note that these tests were performed at shorter residence time compared to the other tests, leading to a lower conversion in each test cycle.) The results, in Fig. 7(b), show that the activity for NO conversion was maintained from the first to the second cycle, clearly indicating that the selectivity loss observed at higher temperatures is due to kinetic effects and not related to deactivation. This result was supported by UV–vis spectroscopy: after the catalytic tests only minor changes were observed in the spectra, suggesting that macroscopic features in terms of clustering are not affected (results not reported for brevity).

Table 2 shows NO conversions obtained over our best catalyst, Fe–NH_4–Z_{40}(O), and over Fe-ZSM-5 catalysts reported in literature. A direct comparison between the results is not straightforward due to different reactions condition used in each case. Especially, the residence time of the gas over the catalyst is shorter in our case than in the literature cases. Even so, the maximum conversion observed at 573 K is highest over our catalyst. At higher temperatures (673 K), the situation changes, due to loss of NO conversion activity for the most active sample in our case, while the most active catalyst tested by Schwidder et al. [46] increases in activity in this temperature range. From 673 to 773 K, the NO conversion decreases over all reported catalysts.

The reason for the different temperature–conversion behaviour between the catalysts is not evident, but could be related to the different O_2 content and/or residence times. Chen et al. [51] showed that O_2 is required for NO reduction to take place, and that the reaction proceeds via NO oxidation to NO_2, followed by adsorption of NO_x species, $x \geq 2$, to Fe sites. The adsorbed species reacts with the hydrocarbon co-reactant to form a NO-containing hydrocarbon polymer species, which subsequently reacts with an incoming NO molecule to form N_2. Chen et al. further observed that at low O_2 partial pressures (less than 2% O_2), the NO conversion rate decreased dramatically. They ascribed this decrease to a build-up of the polymeric species on the active sites, thus blocking the sites active for NO reduction.

For all catalysts, NO reduction as well as hydrocarbon oxidation is observed at all temperatures. With increasing temperatures, the rates of the selective (NO activation) and unselective (direct hydrocarbon oxidation) reactions both increase, as evidenced by an increasing O_2 conversion (not shown). One may speculate that the decrease in NO conversion with increasing temperature is due to a decrease in O_2 concentration along the catalyst bed, leading to blocking of the monomeric sites active for NO reduction, while the oligomeric and clustered sites are still available for hydrocarbon oxidation.

In conclusion, it appears that the catalysts prepared by the new ferric oxalate method have a higher activity for NO activation than the catalysts prepared by the Mohr's salt method. We suggest that the lower NO conversion activity of samples prepared by Mohr salt solution, notwithstanding the high concentration of isolated Fe sites (testified by FTIR, see Fig. 6) is related to the large presence of clusters, detrimental for the catalytic activity.

4. Conclusions

Fe-exchanged ZSM-5 samples with different Si/Al ratios (15, 40 and 140) were prepared with the recently proposed ferric oxalate method. By careful control of proton exchange, performing the exchange at controlled pH, low concentrated samples with high Fe dispersion could be obtained, as testified by FTIR of adsorbed NO and UV–vis experiments. Low Al content in the parent zeolite (Si/Al = 140) lead to catalysts with very low iron amount, relatively large clustering and low activity in the SCR of NO with propane.

Samples with Si/Al = 40 and 15 resulted in highly dispersed iron species, isolated and oligomeric, without a small amount of larger iron oxide clusters. These features result in a high catalytic activity, when compared to literature data and samples prepared by Mohr salt solutions. When ferric oxalate method is used to exchange Na^+-zeolites, the temporary pH increase related to back-exchange of protons causes the formation of hydroxides colloidal solutions responsible for the formation of cluster. This results in lower activity in the NO conversion by propane. Coming to the samples prepared by literature methods, here used as a reference, a higher amount of clusters is observed together with isolated and oligomeric sites. We suggest that the presence of clusters is responsible for the lower activity of the samples, in agreement with previous reports about the detrimental activity of iron oxide clusters in NO reduction, catalyzing competitive oxidation of the reducing agents (propane in this case) [37].

As a conclusion, this work shows that the ferric oxalate method can be used to prepare, easily and in a reproducible manner, catalysts with good activity in the SCR of NO, and that the stability of the catalysts at high temperature can be improved by using high Si/Al ratios in the parent zeolites. This study supports the general picture that isolated, oligomeric and clustered sites can be formed inside the zeolitic channels of ZSM-5 depending upon preparation procedure, and that, while the former is active in SCR, the latter two have a negative effect on NO conversion.

Acknowledgements

Mrs. Sharamala Aravinthan, University of Oslo, is acknowledged for assistance in carrying out the catalytic experiments. The authors acknowledge financial support by Regione Piemonte (Progetto NANOMAT, Docup 2000-2006, Linea 2.4a), EC NoE IDECAT and the Research Council of Norway.

References

[1] G.I. Panov, G.A. Sheveleva, A.S. Kharitonov, V.N. Romannikov, L.A. Vostrikova, Appl. Catal. A Gen. 82 (1992) 31–36.
[2] A.S. Kharitonov, G.A. Sheveleva, G.I. Panov, V.I. Sobolev, Y.A. Paukshtis, V.N. Romannikov, Appl. Catal. A Gen. 98 (1993) 33–43.
[3] G. Berlier, G. Spoto, S. Bordiga, G. Ricchiardi, P. Fisicaro, A. Zecchina, I. Rossetti, E. Selli, L. Forni, E. Giamello, C. Lamberti, J. Catal. 208 (2002) 64–82.
[4] G. Spoto, A. Zecchina, G. Berlier, S. Bordiga, M.G. Clerici, L. Basini, J. Mol. Catal. A Chem. 158 (2000) 107–114.
[5] L.V. Pirutko, V.S. Chernyavsky, A.K. Uriarte, G.I. Panov, Appl. Catal. A Gen. 227 (2002) 143–157.
[6] J. Perez-Ramirez, G. Mul, F. Kapteijn, J.A. Moulijn, A.R. Overweg, A. Domenech, A. Ribera, I. Arends, J. Catal. 207 (2002) 113–126.
[7] P. Fejes, J.B. Nagy, K. Lazar, J. Halasz, Appl. Catal. A Gen. 190 (2000) 117–135.
[8] I. Yuranov, D.A. Bulushev, A. Renken, L. Kiwi-Minsker, J. Catal. 227 (2004) 138–147.
[9] E.J.M. Hensen, Q. Zhu, R.A. van Santen, J. Catal. 233 (2005) 136–146.
[10] W.M. Heijboer, P. Glatzel, K.R. Sawant, R.F. Lobo, U. Bergmann, R.A. Barrea, D.C. Koningsberger, B.M. Weckhuysen, F.M.F. de Groot, J. Phys. Chem. B 108 (2004) 10002–10011.
[11] X.B. Feng, W.K. Hall, J. Catal. 166 (1997) 368–376.
[12] H.Y. Chen, Q. Sun, B. Wen, Y.H. Yeom, E. Weitz, W.M.H. Sachtler, Catal. Today 96 (2004) 1–10.
[13] J. Perez-Ramirez, F. Kapteijn, Appl. Catal. B Environ. 47 (2004) 177–187.
[14] R. Joyner, M. Stockenhuber, J. Phys. Chem. B 103 (1999) 5963–5976.
[15] W.M. Heijboer, A.A. Battiston, A. Knop-Gericke, M. Havecker, H. Bluhm, B.M. Weckhuysen, D.C. Koningsberger, F.M.F. de Groot, Phys. Chem. Chem. Phys. 5 (2003) 4484–4491.
[16] M.S. Kumar, M. Schwidder, W. Grunert, A. Bruckner, J. Catal. 227 (2004) 384–397.
[17] A.Z. Ma, W. Grunert, Chem. Commun. (1999) 71–72.
[18] R.Q. Long, R.T. Yang, R. Chang, Chem. Commun. (2002) 452–453.
[19] B. Wichterlova, Z. Sobalik, J. Dedecek, Appl. Catal. B Environ. 41 (2003) 97–114.
[20] J.A. Sullivan, O. Keane, Appl. Catal. B Environ. 61 (2005) 244–252.
[21] G.S. Qi, R.T. Yang, Catal. Lett. 100 (2005) 243–246.
[22] R.W. Joyner, M. Stockenhuber, Catal. Lett. 45 (1997) 15–19.
[23] G. Delahay, A. Guzman-Vargas, B. Coq, Appl. Catal. B Environ. 70 (2007) 45–52.
[24] P. Marturano, A. Kogelbauer, R. Prins, J. Catal. 190 (2000) 460–468.
[25] J. Perez-Ramirez, M.S. Kumar, A. Bruckner, J. Catal. 223 (2004) 13–27.
[26] E. Hensen, Q.J. Zhu, P.H. Liu, K.J. Chao, R. van Santen, J. Catal. 226 (2004) 466–470.
[27] H.Y. Chen, X. Wang, W.M.H. Sachtler, Appl. Catal. A Gen. 194 (2000) 159–168.
[28] A.A. Battiston, J.H. Bitter, F.M.F. de Groot, A.R. Overweg, O. Stephan, J.A. van Bokhoven, P.J. Kooyman, C. van der Spek, G. Vanko, D.C. Koningsberger, J. Catal. 213 (2003) 251–271.
[29] G. Mul, M.W. Zandbergen, F. Kapteijn, J.A. Moulijn, J. Perez-Ramirez, Catal. Lett. 93 (2004) 113–120.
[30] R.Q. Long, R.T. Yang, Catal. Lett. 74 (2001) 201–205.
[31] L.J. Lobree, I.C. Hwang, J.A. Reimer, A.T. Bell, J. Catal. 186 (1999) 242–253.
[32] I. Melian-Cabrera, F. Kapteijn, J.A. Moulijn, Chem. Commun. (2005) 2178–2180.
[33] K.A. Dubkov, N.S. Ovanesyan, A.A. Shteinman, E.V. Starokon, G.I. Panov, J. Catal. 207 (2002) 341–352.
[34] A. Zecchina, M. Rivallan, G. Berlier, C. Lamberti, G. Ricchiardi, Phys. Chem. Chem. Phys. 9 (2007) 3483–3499.
[35] J.F. Jia, Q. Sun, B. Wen, L.X. Chen, W.M.H. Sachtler, Catal. Lett. 82 (2002) 7–11.
[36] F. Heinrich, C. Schmidt, E. Loffler, M. Menzel, W. Grunert, J. Catal. 212 (2002) 157–172.
[37] M. Schwidder, F. Heinrich, M.S. Kumar, A. Bruckner, W. Grunert, Stud. Surf. Sci. Catal. 154 (2004) 2484–2492.
[38] E.V. Kondratenko, J. Perez-Ramirez, Catal. Today 119 (2007) 243–246.
[39] K.Q. Sun, H. Xia, E. Hensen, R. van Santen, C. Li, J. Catal. 238 (2006) 186–195.
[40] L. Kiwi-Minsker, D.A. Bulushev, A. Renken, J. Catal. 219 (2003) 273–285.
[41] G. Centi, C. Genovese, G. Giordano, A. Katovic, S. Perathoner, Catal. Today 91–92 (2004) 17–26.
[42] E.J.M. Hensen, Q. Zhu, M. Hendrix, A.R. Overweg, P.J. Kooyman, M.V. Sychev, R.A. van Santen, J. Catal. 221 (2004) 560–574.
[43] N. Hansen, A. Heyden, A.T. Bell, F.J. Keil, J. Phys. Chem. C 111 (2007) 2092–2101.
[44] G. Berlier, G. Ricchiardi, S. Bordiga, A. Zecchina, J. Catal. 229 (2005) 127–135.
[45] G.D. Pirngruber, M. Luechinger, P.K. Roy, A. Cecchetto, P. Smirniotis, J. Catal. 224 (2004) 429–440.
[46] M. Schwidder, M.S. Kumar, A. Bruckner, W. Grunert, Chem. Commun. (2005) 805–807.
[47] G. Berlier, A. Zecchina, G. Spoto, G. Ricchiardi, S. Bordiga, C. Lamberti, J. Catal. 215 (2003) 264–270.
[48] I. Melian-Cabrera, F. Kapteijn, J.A. Moulijn, Catal. Today 110 (2005) 255–263.
[49] M.T. Nechita, G. Berlier, G. Ricchiardi, S. Bordiga, A. Zecchina, Catal. Lett. 103 (2005) 33–41.
[50] D.A. Bulushev, L. Kiwi-Minsker, A. Renken, J. Catal. 222 (2004) 389–396.
[51] H.Y. Chen, T. Voskoboinikov, W.M.H. Sachtler, J. Catal. 180 (1998) 171–183.
[52] H.Y. Chen, T. Voskoboinikov, W.M.H. Sachtler, J. Catal. 186 (1999) 91–99.
[53] A.W.L. Dudeney, I.I. Tarasova, Hydrometallurgy 47 (1998) 243–257.
[54] D. Panias, M. Taxiarchou, I. Douni, I. Paspaliaris, A. Kontopoulos, Can. Metall. Quart. 35 (1996) 363–373.
[55] S.O. Lee, T. Tran, J. BH, S.J. Kim, M.J. MKim, Hydrometallurgy 87 (2007) 91–99.
[56] M. Taxiarchou, D. Panias, I. Douni, I. Paspaliaris, A. Kontopoulos, Hydrometallurgy 44 (1996) 219–230.
[57] E. Christodoulou, D. Panias, I. Paspaliaris, Can. Metall. Quart. 40 (2001) 421–432.
[58] M. Trombetta, G. Busca, S. Rossini, V. Piccoli, U. Cornaro, A. Guercio, R. Catani, R.J. Willeyz, J. Catal. 179 (1998) 581–596.
[59] S. Bordiga, E.E. Platero, C.O. Arean, C. Lamberti, A. Zecchina, J. Catal. 137 (1992) 179–185.
[60] S. Bordiga, R. Buzzoni, F. Geobaldo, C. Lamberti, E. Giamello, A. Zecchina, G. Leofanti, G. Petrini, G. Tozzola, G. Vlaic, J. Catal. 158 (1996) 486–501.
[61] M. Santhosh Kumar, M. Schwidder, W. Grunert, U. Bentrup, A. Bruckner, J. Catal. 239 (2006) 173.
[62] L. Capek, V. Kreibich, J. Dedecek, T. Grygar, B. Wichterlova, Z. Sobalik, J.A. Martens, R. Brosius, V. Tokarova, Microporous Mesoporous Mater. 80 (2005) 279–289.
[63] M.W. Simon, S.S. Nam, W.Q. Xu, S.L. Suib, J.C. Edwards, C.L. Oyoung, J. Phys. Chem. 96 (1992) 6381–6388.
[64] G. Lehmann, Z. Phys. Chem. Neue Folge 72 (1970) 279.
[65] G. Berlier, G. Spoto, G. Ricchiardi, S. Bordiga, C. Lamberti, A. Zecchina, J. Mol. Catal. A Chem. 182 (2002) 359–366.
[66] A.S. Kumar, J. Perez-Ramirez, M.N. Debbagh, B. Smarsly, U. Bentrup, A. Bruckner, Appl. Catal. B Environ. 62 (2006) 244–254.
[67] K. Krishna, G.B.F. Seijger, C.M. van den Bleek, M. Makkee, G. Mul, H.P.A. Calis, Catal. Lett. 86 (2003) 121–132.
[68] M. Lezcano, V.I. Kovalchuk, J.L. d'Itri, Kinet. Catal. 42 (2001) 104–111.
[69] G. Mul, J. Perez-Ramirez, F. Kapteijn, J.A. Moulijn, Catal. Lett. 80 (2002) 129–138.
[70] K. Hadjiivanov, J. Saussey, J.L. Freysz, J.C. Lavalley, Catal. Lett. 52 (1998) 103–108.
[71] K. Hadjiivanov, A. Penkova, M. Daturi, J. Saussey, J.C. Lavalley, Chem. Phys. Lett. 377 (2003) 642–646.
[72] G. Berlier, C. Prestipino, M. Rivallan, S. Bordiga, C. Lamberti, A. Zecchina, J. Phys. Chem. B 109 (2005) 22377–22385.
[73] B.R. Wood, J.A. Reimer, A.G. Bell, J. Catal. 209 (2002) 151–158.
[74] G. Spoto, S. Bordiga, D. Scarano, A. Zecchina, Catal. Lett. 13 (1992) 39–44.
[75] L.J. Lobree, I.-C. Hwang, J.A. Reimer, A.T. Bell, Catal. Lett. 63 (1999) 233–240.